Optical Materials 42 (2015) 381–384

Contents lists available at ScienceDirect

Optical Materials

journal homepage: www.elsevier.com/locate/optmat

Photoluminescence and radioluminescence properties of MnO-doped SnO–ZnO–P_2O_5 glasses

Hirokazu Masai [a,*], Yusuke Hino [a], Takayuki Yanagida [b], Yutaka Fujimoto [b,1]

[a] Institute for Chemical Research, Kyoto University, Gokasho, Uji, Kyoto 611-0011, Japan
[b] Kyushu Institute of Technology, 2-4 Hibikino, Wakamatsu-ku, Kitakyushu 808-0196, Japan

ARTICLE INFO

Article history:
Received 21 October 2014
Received in revised form 24 December 2014
Accepted 16 January 2015
Available online 7 February 2015

Keywords:
Photoluminescence
Radioluminescence
Glass
Sn^{2+}
Mn^{2+}

ABSTRACT

In this study, the photoluminescence and radioluminescence properties of MnO-doped SnO–ZnO–P_2O_5 glasses are examined. We have confirmed that linear dose-dependence and radioluminescence emission decay depend on Mn^{2+} concentration. Energy transfer from donor Sn^{2+} center to acceptor Mn^{2+} center is observed in both photoluminescence and radioluminescence processes, and the energy transfer efficiency is more than 90% when the Mn^{2+}/Sn^{2+} ratio is 5. Since emission intensity of Mn^{2+} is higher than that of Sn^{2+} in radioluminescence compared to photoluminescence, it is suggested that energy transfer from the host matrix to Mn^{2+} center by X-ray occurred preferentially over energy transfer to Sn^{2+} center. The present results suggest that the conventional parity rule for photoluminescence is not always adaptable for radioluminescence, although emission-related energy levels are the same for both the processes.

1. Introduction

Oxide glass is a fundamental industrial material that exhibits good transparency, wide chemical composition range, and good formability. Owing to its high chemical durability, practical applications of oxide glass have been constantly examined from both industrial and academic viewpoints. Despite the presence of several reports on rare earth (RE)-containing bulk glass [1–3], RE-free phosphors are in demand because of the uneven distribution of RE elements on earth. Therefore, we focus on the ns^2-type (n = 4, 5, 6) ions as emission centers. These ions exhibit an outer shell electronic configuration of ns^2 in the ground state and ns^1np^1 in the excited state. Sn^{2+}, Sb^{3+}, Tl^{+}, Pb^{2+}, and Bi^{3+} are well-known examples of the same [4–8]. Although these ions as emission centers exhibit generally parity-allowed transition, their emission properties in glass materials have not been examined or documented properly owing to their metastable valencies.

We have previously reported the highest quantum efficiency (QE) of photoluminescence (PL) for amorphous SnO–ZnO–P_2O_5 (SZP) low-melting glass [9]. It is notable that the transparent oxide glass containing no RE cation shows strong UV-excited emission that is comparable to that exhibited by crystal phosphors such as $MgWO_4$; further, this was the largest reported QE of a glass material without RE cation. More recently, we have also demonstrated the UV-excited white light emission property of MnO-codoped SZP glasses [10,11]. The broad-band white light emission can be tailored by addition of Mn^{2+} ions instead of RE ions as emission centers. Recently, we have reported that Sn^{2+}-Mn^{2+} cluster-like structures, which are predicted in Sn^{2+}- and Mn^{2+}-codoped alkali halide crystals [12–14], may be generated even in the random glass network from the viewpoint of high ET efficiency [15]. As SnO-doped zinc phosphate glasses showed radioluminescence (RL) under X-ray irradiation or charged-particle irradiation [16,17], MnO-codoped samples are also expected to show good scintillation properties.

PL properties of various transition metal-doped solid-state materials as well as RL properties of several systems, such as crystal and ceramics [18], and glasses [19] are reported. However, the correlation between PL and RL of a donor–acceptor system has not been clarified yet. In this study, we examined the PL and RL properties of MnO-doped SZP glasses, and discussed the corresponding emission mechanisms.

2. Experimental

The MnO-doped SZP glasses were prepared by the conventional melt-quenching method. Nominal chemical compositions of the xMnO–1SnO–59ZnO–40P_2O_5 glasses are reported in units of mol%. Herein, the general glass system is designated as xMn–1SZP

* Corresponding author. Tel.: +81 774 38 3131; fax: +81 774 33 5212.
E-mail address: masai_h@scl.kyoto-u.ac.jp (H. Masai).
[1] Present address: Department of Applied Chemistry, Tohoku University, 6-6-07 Aoba, Sendai 980-8579, Japan.

http://dx.doi.org/10.1016/j.optmat.2015.01.031
0925-3467/

glass. The preparation scheme under air-conditioning is previously reported [20]. After quenching and annealing at the glass-transition temperature (T_g), the glass sample was cut to dimensions of 10 mm × 10 mm × 1 mm and mechanically polished using diamond slurry. The T_g was measured by differential thermal analysis (DTA, Thermo Plus 8120, Rigaku) at a heating rate of 10 °C/min. PL and PL excitation (PLE) spectra were recorded using a fluorescence spectrophotometer (F-7000, Hitachi). PL decay curves were measured using a compact fluorescence lifetime spectrometer (Quantaurus-Tau, Hamamatsu Photonics). RL spectra by X-ray radiation at room temperature were recorded using a monochromator equipped with a charge-coupled device (CCD, Andor DU-420-BU2) [21]. The supplied bias voltage and tube current were 40 kV and 0.052–5.2 mA, respectively. The irradiated dose was calibrated using an ionization chamber. RL decay curves were recorded using a pulse X-ray tube (Hamamatsu N5084) and a photomultiplier tube (Hamamatsu R7400) as the photodetector [22]. The system was conceptually similar to a pulse X-ray streak camera system [23], with a different photodetector.

3. Results and discussion

Fig. 1 shows the optical absorption spectra of *x*Mn–1SZP glasses containing different amounts of MnO. The inset shows a photograph of these glasses. The fact that there is no significant change in these optical absorption edges, shows that the absorption edges are constituted of s–p transition of Sn^{2+} species that is not affected by the existence of Mn^{2+}, in the given concentration range. Manganese is known to exist as Mn^{2+} or Mn^{3+} in zinc phosphate glasses [24]. The absence of a clear absorption band due to Mn^{3+} [25,26] in the whole measured region shows that only Mn^{2+} exists in these glasses. Fig. 2 shows the PL emission spectra of the *x*MnO–1SZP glasses. Excitation energy is 4.6 eV corresponding to the PLE peak of Sn^{2+} center. The emission intensity at 3.1 eV, due to emission of Sn^{2+} center, decreases with increasing amount of MnO whereas the intensity at 2.0 eV, attributed to emission of Mn^{2+} center, increases. There are insignificant changes (less than 0.1 eV) to the emission peaks and the width of the emission band of Sn^{2+} center, after deconvolution. It suggests that the local coordination field, *i.e.* emission-related energy levels, of Sn^{2+} center is not affected by the addition of Mn^{2+}. The emission band of SZP glass correlates to the optical absorption edge [27,28]. The observed PL peak positions' being independent of the Mn^{2+} content is consistent with the optical absorption band shown in Fig. 1.

Fig. 3 shows the PL decay curves of the Sn^{2+} emission center excited by a photon of energy of 4.43 eV. The decay curves indicate that the almost single exponential decays of Sn^{2+} emission center become non-exponential on addition of MnO, and that the decay

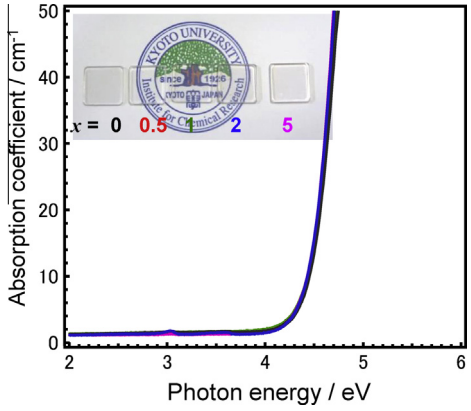

Fig. 1. Optical Absorption spectra of *x*MnO–1SZP glasses (x = 0, 0.5, 1, 2, and 5). Inset shows a photograph of these glasses.

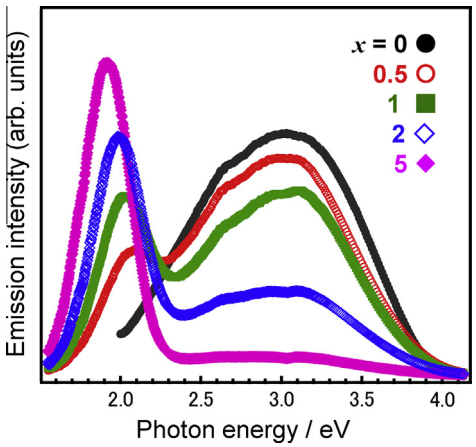

Fig. 2. PL emission spectra of *x*MnO–1SZP glasses. Excitation energy is 4.6 eV corresponding to the PLE peak of Sn^{2+} center.

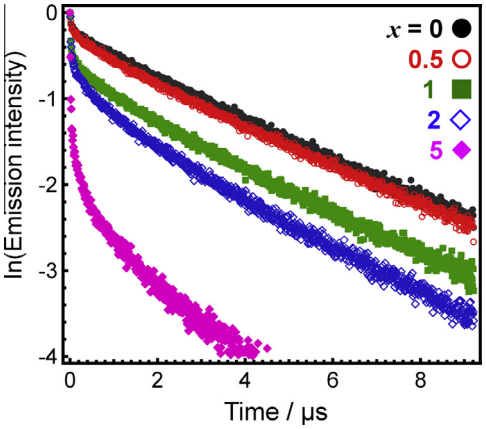

Fig. 3. PL decay curves of Sn^{2+} center of *x*MnO–1SZP glasses. The photon energies of excitation and emission are 4.4 and 3.1 eV, respectively.

constant of Sn^{2+} decreases with increasing MnO content. The decrease of both PL intensity and emission decay of Sn^{2+} center clearly suggests energy transfer (ET) from Sn^{2+} to Mn^{2+} centers during the PL process. For quantitative discussion, we focus on the decay constant ($\tau_{1/e}$) of donor Sn^{2+} center of these glasses. ET efficiency (η_{ET}) in the emission process is given by Eq. (1) [29],

$$\eta_{ET} = 1 - \frac{\tau_{D,A}}{\tau_D} \quad (1)$$

where $\tau_{D,A}$ and τ_D are decay constants of Sn^{2+} center, with and without acceptor Mn^{2+} cation, respectively. Fig. 4 shows the PL decay constant and the ET efficiency as functions of MnO content in the *x*Mn–1SZP glasses. ET efficiency increases with increasing MnO content, and the value is over 90% when MnO content is more than 4 mol%. The high ET rate in the present study suggests formation of a Sn^{2+}–Mn^{2+} cluster-like structure, corroborated by another study [15].

Fig. 5 shows the X-ray induced scintillation spectra of the *x*MnO–1SZP glasses and the variation of emission intensity of Mn^{2+} center (~2.1 eV) with varying MnO content. Although there are small shifts (~0.1 eV) in emission peaks between PL and RL spectra, it is difficult to discuss the origin of the shifts. Therefore, it is natural to assume that emission-related energy levels of the PL and RL processes are the same. Compared to the PL emission spectra (Fig. 2), the emission intensity ratio between Sn^{2+} and Mn^{2+} is different in RL, due to the difference in excitation processes.